DonnishJournals 2041-3165

Donnish Journal of Pure And Applied Chemistry
Vol 1(1) pp. 008-019 April, 2015
http://www.donnishjournals.org/djpac

Original Research Article

Study of Ca^{2+}, K^{+}, and Fe^{3+} ions Influence on Struvite Precipitation from Synthetic Water by Dissolved CO_2 Degasification Technique

[1,2,3]Hassidou Saidou*, [2,3]Atef Korchef, [2]Sami Ben Moussa and [2]Mohamed Ben Amor

[1]Department of Chemistry, Faculty of Sciences and Techniques, University of Maradi, Niger.
[2]Laboratory of Natural Water Treatment, Water Research and Technology Centre, Technopark of Borj-Cedria, Tunisia.
[3]Laboratory of Valorization of Useful Materials, National Centre of Research in Material Sciences, Technopark of Borj-Cedria, Tunisia.

Accepted 20th March, 2015.

The influence of Ca^{2+}, K^{+}, and Fe^{3+} on struvite precipitation was investigated in this study, by dissolved CO_2 degasification technique. The results obtained showed that increasing the calcium ions improved phosphates removal efficiency and the precipitated solid changes from crystalline phase (struvite) to an amorphous one, identified as $Ca_9(PO4)_6 \cdot nH_2O$ from an initial Ca^{2+} concentration of 4 mM. However, the formation of this amorphous phase preceded the struvite formation in the Ca^{2+} concentration range of [2.5 -3.5 mM]. The increase in Ca^{2+} concentration from 2 to 4 mM approaches a homogeneous distribution of the average particle size. Increasing the concentration of K^{+} improves phosphates removal yield, and did not affect the purity of the struvite obtained. The introduction of Fe^{3+} in the solution causes enormous change both on physicochemical parameters and on the morphology of the precipitate obtained. Indeed, the increase in the molar ratio destroyed struvite crystallization immediately and formed an amorphous phase identified as $FePO_4 \cdot 2H_2O$ at pH 6.5 and Fe^{3+}/PO_4^{3-} molar ratio ≥ 1. Furthermore, the presence of Fe^{3+} promoted the increasing particle size of the two phases (crystalline and amorphous). It should be noted that the yield of phosphate removal is better when forming the amorphous phase.

Keywords: Dissolved CO_2 degasification technique, Synthetic water, Struvite, Ca^{2+}, K^{+}, Fe^{3+}

INTRODUCTION

Phosphate and ammonium ions can be recovered simultaneously by magnesium through precipitation of the sparingly soluble magnesium ammonium phosphate salt, known as struvite ($MgNH_4PO_4 \cdot 6H_2O$) (Diwani et al., 2007; Saidou et al., 2009a; Zhang et al., 2009). This is possible, at relatively short time, by the dissolved CO_2 degasification technique (Saidou et al., 2009a). Therefore, struvite can be obtained from different kinds of wastewater containing an important amount of phosphate and ammonium ions, like leachate (Saidou et al., 2010; Huang et al., 2014a,b; Lahav et al., 2013). As phosphates and ammonium ions are nutritious for crops, struvite recovered can be used as a valuable mineral fertilizer in agriculture (Brigder, 2001; De-Bashan and Bashan, 2004). Even so, struvite can also contribute to scale formation in wastewater treatment equipments (Borgerding, 1972; Webb and Ho, 1992; Saidou et al., 2009b), and this phenomenon can be prevented by reducing total phosphates availability via ferric chloride addition (Mudragada et al., 2014).

Otherwise, struvite precipitation is controlled by several key parameters such as pH (Saidou et al., 2009a; Saidou et al.,

Corresponding Author: saidouhassidou@gmail.com

2009b; Ben Moussa et al., 2011; Le Corre et al., 2005). The study of Zhelong et al. (2014), showed that struvite aggregates was formed in relatively low phosphorus concentration between 3.0 and, 5.0 mmol/L and mildly alkaline conditions (pH 9.0 – 9.5). Kozic et al. (2014) have found that increase in pH from 8.5 to 10 in struvite reaction crystallization environment produced a decrease in mean crystal size by about 44% on average. The same observation was done by Hutnik et al. (2013). There are many studies about the impact of foreign ions on struvite earlier [15, 19].

For examples Muryanto and Bayuseno (2014), did not observe any significant change in the morphology of struvite obtained, by the addition of Cu^{2+} and Zn^{2+} ions. Several works about the influence of some ions have been focused by other techniques, but there are few studies about the influence of some ions by the CO_2 degasification technique (Saidou et al., 2009a). The aim of this study is to investigate the influence of Ca^{2+}, K^{+}, and Fe^{3+} ions on struvite precipitation by this technique (Saidou et al., 2009a).

MATERIAL AND METHODS

Solutions preparation

Synthetic water used in all experiments in this work was prepared by mixing the respective aqueous solutions of $MgCl_2{\cdot}6H_2O$ and $NH_4H_2PO_4$ in desired proportions in a calcium carbonate solution. The latter was previously prepared by dissolving calcium carbonate solids in a flow of CO_2. Reagents $MgCl_2.6H_2O$ (purity> 99%), $NH_4H_2PO_4$ (purity> 99%) and $CaCO_3$ (purity 99%) were respectively supplied by Fluka, Sigma Aldrich and Merck.

The study of the influence of calcium, potassium and iron ions was performed using solutions prepared from KCl, $CaCO_3$, and $FeCl_2{\cdot}7H_2O$. The calcium ions were added in synthetic solution at a concentration varying from 0 to 4mM. Potassium and iron ions were introduced at molar ratios in the intervals [0, 8] and [0, 2], respectively. It should be noted that all these experiments are conducted at 25 ° C, an airflow rate of 40 $L.min^{-1}$, an initial solution pH of 6.5 in a PVC cell by the dissolved CO_2 degasification technique (Saidou et al., 2009a).

Analysis

The phosphate concentration in the solution was determined by the colorimetric method using the reagent vanadomolybdic UV-visible spectrophotometer. The precipitated solids obtained were analyzed using different physicochemical techniques: X-rays diffraction (XRD), scanning electron microscopy (SEM), infrared (IR), laser particle size, differential scanning calorimetry (DSC).

RESULTS AND DISCUSSION

Study of Ca^{2+} ions influence

In the absence of calcium ions, and therefore the CO_2 from their dissolution, in the solution, the pH of the solution increases rapidly and stabilized at a value of 6.7. In this case, no precipitation was detected since the pH value does not reach 8.1 found in the previous study (Saidou et al., 2009a). The increase in Ca^{2+} concentration in the solution affected the temporal evolution of the pH. However, it should be noted that the drop in pH is remarkable only for calcium concentration between 0.5 and 2 mM (Fig. 1).

The temporal evolution of PO_4^{3-} concentration is shown in Fig. 2. The induction time is lower (about 10 min) for Ca^{2+} concentration varying between 2 to 3 mM. But, these times are much higher than those reported in the literature, especially the study of Kabdasli et al. (2006). Indeed, the precipitation of struvite is detected only from 57 seconds (<15 min in this work) when $[Ca^{2+}] = 0.5$ mM.

This difference is probably due to the method used, since the experiments performed by these authors are by magnetic stirring and not by the CO_2 degasification technique used in this study. Furthermore, this short time (close to the one found by Kabdasli et al. (2006) was obtained in our previous work with solutions of initial pH of 8 (Saidou et al., 2009a). The yield of phosphorus removal generally increases when the concentration of Ca^{2+} increases. It reaches its maximum at 72% for Ca^{2+} concentration of 3.5 mM. Moreover, it is found that 50% of phosphate was recovered for less than 20 min for this calcium ions concentration (Fig. 2).

From the X-ray diffractograms of the precipitates (Fig. 3) and the IR spectrum (Fig. 4) of amorphous precipitate obtained for Ca^{2+} concentration of 4 mM, we noted that the addition of calcium ions promoted the precipitation and affects the purity of struvite obtained. The latter observation is supported by the diffraction patterns of the solids obtained after 90 minutes of reaction time. Indeed, the precipitated solid is crystallized for the calcium ions concentration from 0.5 to 3.7 mM. It was identified as struvite. However, the precipitated solid is amorphous when the calcium ions concentration reached 4 mM, corresponding to Mg^{2+}/Ca^{2+} molar ratio equal to 1.

This amorphous solid has an X-ray diffractogram and IR spectrum similar to amorphous hydrated calcium phosphate ($Ca_9(PO_4)_6{\cdot}nH_2O$) ones, reported by several works of literature (Walleys, 1952; Heughebaert and Montell, 1977; Zahidi, 1984; Zahidi et al., 1985; Banu, 2005). In fact, this compound is characterized by a large peak centered at $2\theta = 36.5$ ° (λCo) and by the absence of any other diffraction streak that may correspond to a crystalline phase. This observation is partially in agreement with the results of Le Corre et al., (2005) showing the simultaneous presence of two phases (crystalline and amorphous) at the same molar ratio Mg^{2+}/Ca^{2+}

We have seen an evolution of the crystallized solid precipitate to the amorphous phase by increasing the concentration of Ca^{2+}. The question which can be asked now is: Was crystallization the result of an evolution of the amorphous phase during the degasification time?

Indeed, the CO_2 degasification was stopped after 15 minutes reaction time. The precipitates obtained after filtration of the mixture were analyzed by XRD, and showed the presence of an amorphous phase. The filtrate was then degassed for 75 minutes reaction time. A crystalline phase appeared, independently of the calcium ions concentration studied. This study showed that, when spreads degasification time, the precipitated solid changed from amorphous phase to crystalline phase (Fig. 5).

Furthermore, the morphology of solids obtained from mixtures containing calcium ions concentration of 0.5, 2.5 and 4 mM was analyzed by SEM (Fig. 6 a, b, c). Thus, as the Ca^{2+} concentration increased, the more shapes "sticks" characteristics of struvite decreased to disappear at the end, for the calcium ions concentration of 4 mM. This is confirmed by the analysis of a grain of solid obtained by EDAX (Fig. 6 a ', b', c ').

To evaluate the influence of calcium on the particles size of the precipitated solid, particle size analysis was performed and the results showed that the evolution of the particles size according to their proportion revealed two maxima whose

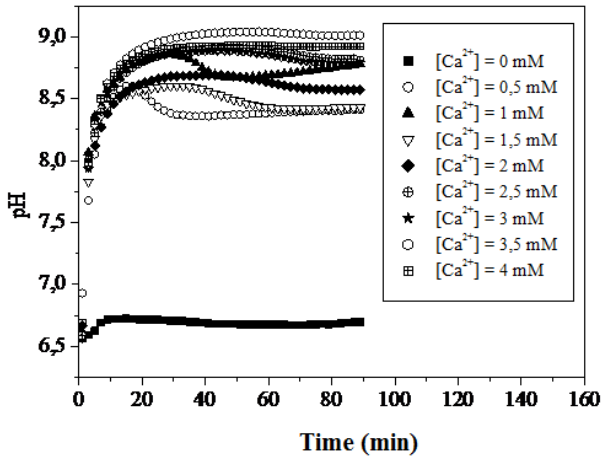

Fig. 1. Evolution of solution pH during time with different Ca^{2+} concentration

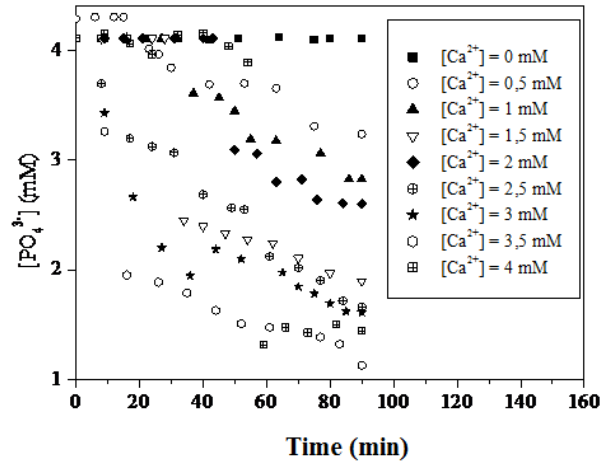

Fig. 2. Temporal evolution of PO_4^{3-} concentration, for different Ca^{2+} concentration

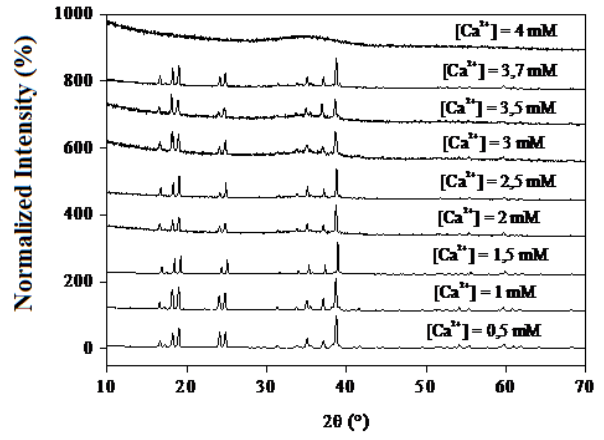

Fig. 3. Superposition of X-rays diffractograms of precipitates obtained for different calcium ions concentration

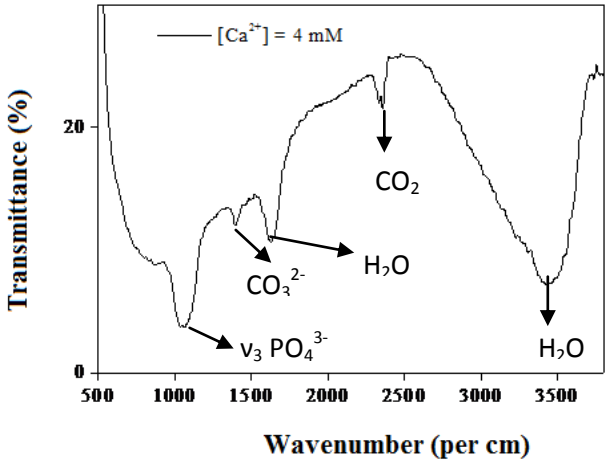

Fig. 4. Infrared spectrum of precipitate obtained for calcium ions concentration of 4 mM

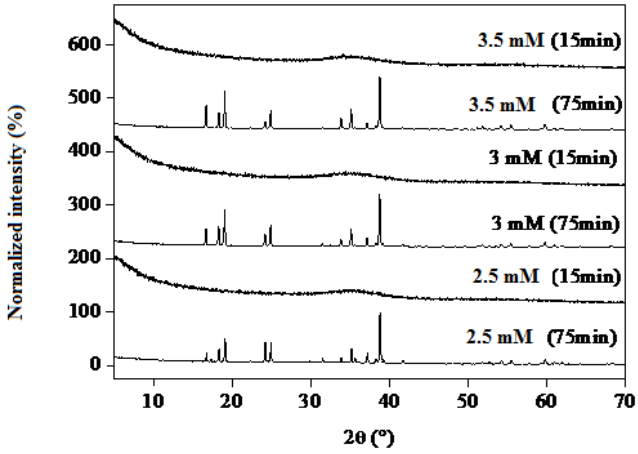

Fig. 5. Superposition of X-rays diffractograms of solids obtained after 15 min and 75 min reaction time for calcium ions concentration of: 2.5, 3, and 3.5 mM

values are located at about 8 microns and 69 microns for Ca^{2+} concentration about 1.5 mM (Fig. 7). An increase in the concentration of Ca^{2+} from 2 to 4 mM approaches an homogeneous distribution of the particles average size of the order of 10 microns for a Mg^{2+} /Ca^{2+} = 1 ([Ca^{2+}] = 4 mM) with the presence of a small number of particle size between 50 and 280 microns. These results differed from those obtained in the literature (Le Corre et al., 2005) whose sizes ranged from 2.15 to 3.10 microns. This difference is probably due to the experimental reaction time from which the particle size analysis was performed. In fact, these authors showed that after 20 min of reaction, the two groups are respectively 50 and 1000 microns for the same molar ratio.

Furthermore, most of the grains formed are small sizes of the order of 10 microns extending in preferred directions over time to form the crystallized phases. They are presented as two sub-groups and equivalent number average sizes of about 50 and 100 microns (Fig. 8).

Study of K^+ ions influence

Temporal changes in pH (Fig. 9) and PO_4^{3-} concentration (Fig. 10) showed that the addition of potassium ions in the solution does not affect the precipitation phenomenon since the shape of the curve pH = f (t) has the same form as in the previous case. Its influence was noticed firstly, on the precipitation pH ranging from 8.3 to 8.7 depending on the K^+/PO_4^{3-} molar ratio and secondly, on the induction time, which decreased from 35 to 19 min for K^+/PO_4^{3-} molar ratio from 0 to 1.

Beside it increased when exceeding the upper limit of 1 and reached 31 minutes for K^+/PO_4^{3-} molar ratio of 8. In addition, the yield of phosphates removal evolved generally in the same direction as K^+/PO_4^{3-} molar ratio, except when it reached the value of 8 when a slight decrease about 51%, was detected.

Moreover, another phase may be co-precipitated with struvite in small amounts and probably comes from the substitution of a portion of Mg^{2+} and / or NH_4^+ by K^+. This deduction came from:

Firstly, the change in intensity of some peaks in the diffractograms (decrease:) or (increase:), detected from K^+/PO_4^{3-} molar ratio of 1 (Fig. 11).

Secondly, the difference in heights corresponding to the various elemental constituents of precipitated product (Fig. 12).

The results of particle size analysis of the precipitates obtained for PO_4^{3-} concentration of 3.8 mM and various

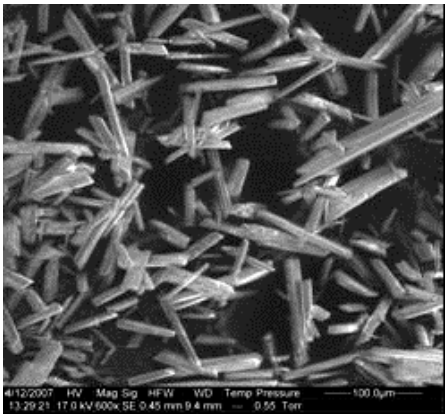

(a)

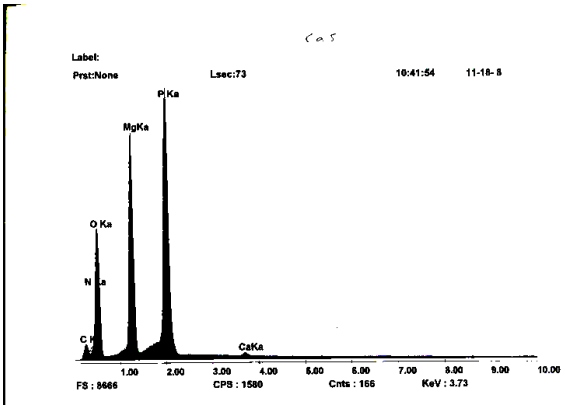

(a')

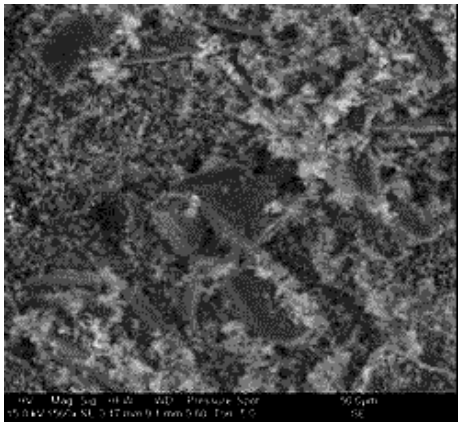

(b)

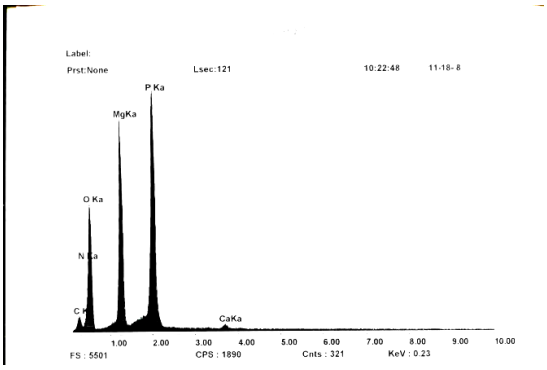

(b')

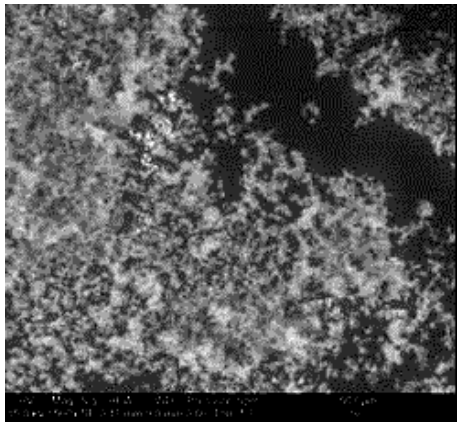

(c)

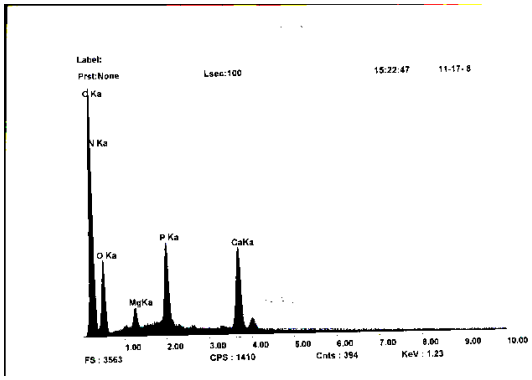

(c')

Fig. 6. SEM and EDAX and spectra corresponding precipitates for (a, a ') $[Ca^{2+}]$ = 0.5 mM (b, b') $[Ca^{2+}]$ = 2.5 mM, (c, c') $[Ca^{2+}]$ = 4 mM

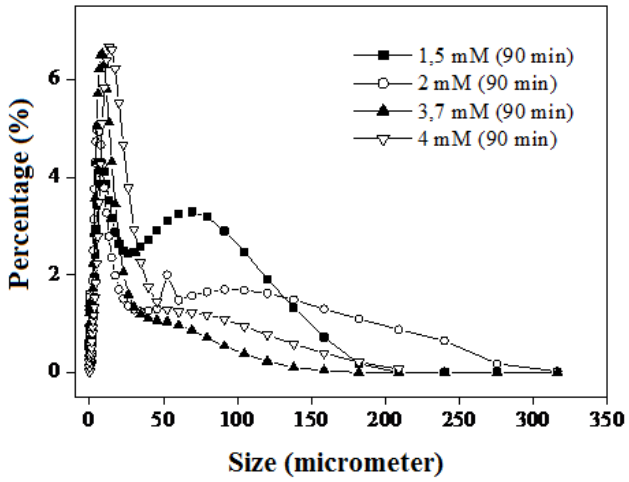

Fig. 7. Percentage of particle size obtained after 90 min reaction time for different calcium ions concentration

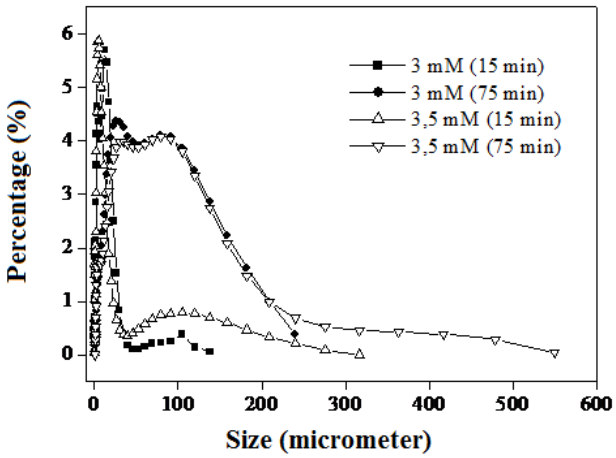

Fig. 8. Percentage of particle size obtained after 15 and 75 min. reaction time for different calcium ions concentration

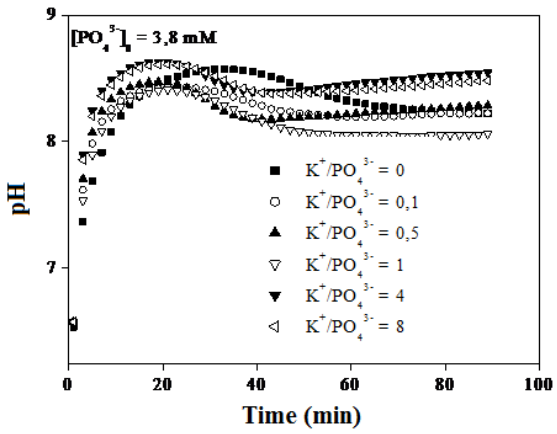

Fig. 9. Temporal evolution of solution pH at different K^+/PO_4^{3-} molar ratios

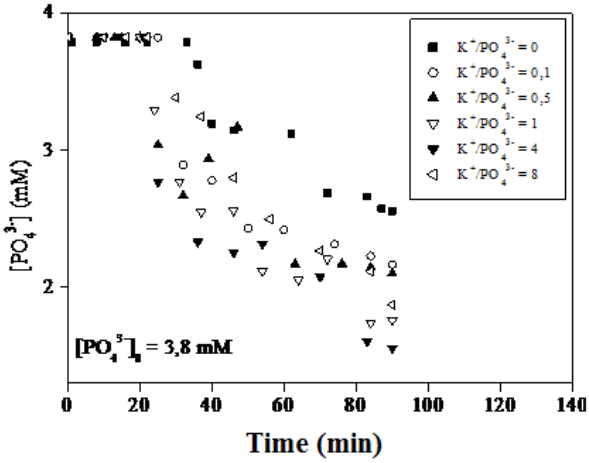

Fig. 10. Temporal evolution of solution PO_4^{3-} ions concentration at different K^+/PO_4^{3-} molar ratios

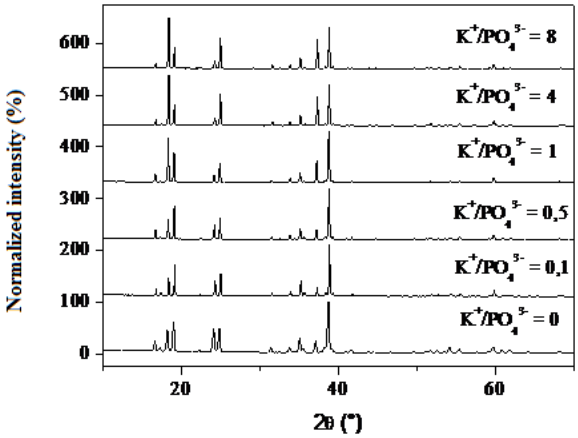

Fig. 11. Superposition of X-rays diffractograms at different K^+/PO_4^{3-} molar ratios

K^+/PO_4^{3-} molar ratios are given in Fig. 13. We noted that the increase in K^+/PO_4^{3-} molar ratio promoted crystal growth to an average value of 50 microns and raising their proportion depending on the molar ratio.

Study of Fe^{3+} ions influence

The results of the X-rays diffraction analysis (Fig. 14) of precipitates formed, the SEM photography (Fig. 15), the elemental analysis (spectra) EDAX (Fig. 15), the particle size distribution of the precipitates (Fig. 16), the temporal evolution of the solution pH (Fig. 17) and the time course of PO_4^{3-} concentration in solution (Fig. 18) allowed us to deduce the physicochemical characteristics summarized in Table 1.

The introduction of iron ions in the solution causes huge changes both on the physicochemical parameters and on the morphology of the precipitate obtained (Fig 14 and Fig. 15). Indeed, the increase in the molar ratio destroyed struvite crystallization and formed an amorphous phase observed for $Fe^{3+}/PO_4^{3-} \geq 1$ as shown by the X-rays analysis of Figure 14. This amorphous phase is identified as hydrated iron phosphate ($FePO_4 \cdot 2H_2O$). This result is in agreement with the study of Zhang et al. (2010) and justified by elemental analysis showing the predominance of iron element at the expense of Mg (Fig. 15). In addition, increasing the particle size of the two phases (crystalline and amorphous) is promoted in the presence of iron. Most of the latter has an average size of about 1000 to 1500 micron (Fig. 16).

Moreover, it is noted that the amorphous phase is obtained immediately after the addition of iron (induction time < 1 min) at a slightly acidic pH of 6.5 (Fig. 17) indicating the absence of the precipitation of struvite (Fig. 18). This is confirmed by a disappearance of the shapes of the needle characteristic of struvite for Fe^{3+}/PO_4^{3-} molar ratio from 0.1 to 1, as shown by the SEM pictures. It should be noted that the yield of phosphate removal is better when forming amorphous phase, since it reached a removal rate of approximately 95% (Table 1). This result is in agreement with the work of Zhang et al. (2010).

It should also be noted that the formation of $FePO_4 \cdot 2H_2O$ disadvantage scaling of the material used, since the largest amount of solid precipitated in solution.

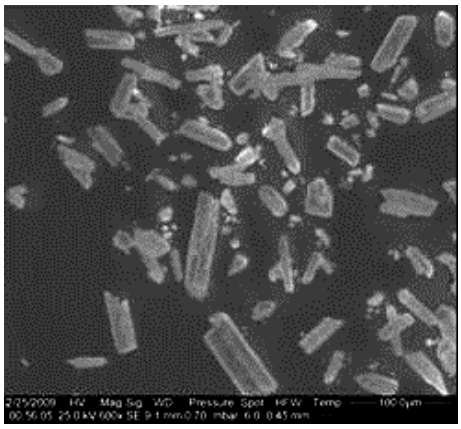

(a)

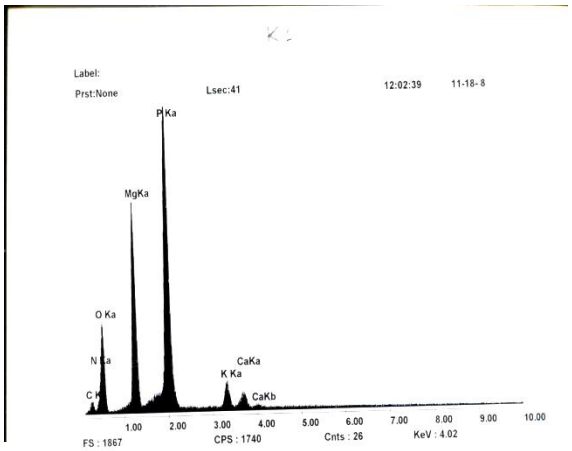

(a)'

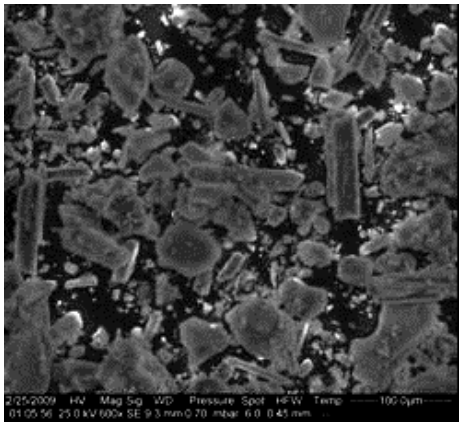

(b)

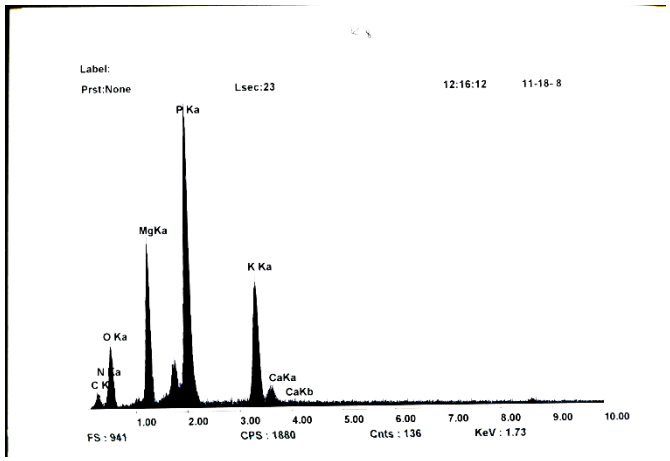

(b')

Fig. 12. EDAX spectra and SEM photography of the obtained crystals (a, a '): K^+/PO_4^{3-} = 1, (b, b'): K^+/PO_4^{3-} = 8

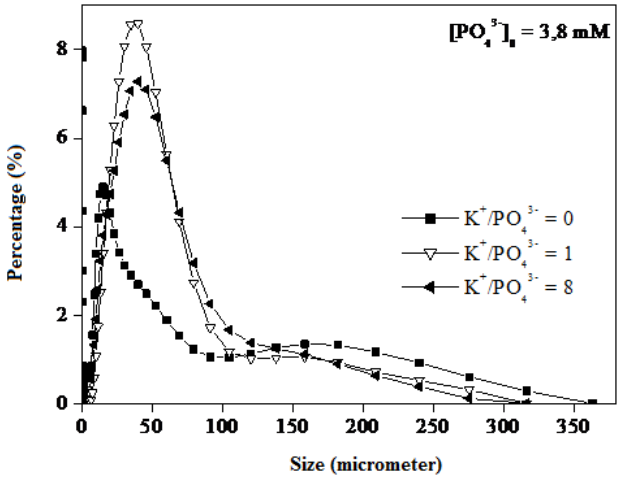

Fig. 13. Percentage of particle size of precipitates obtained for different K^+/PO_4^{3-} molar ratios

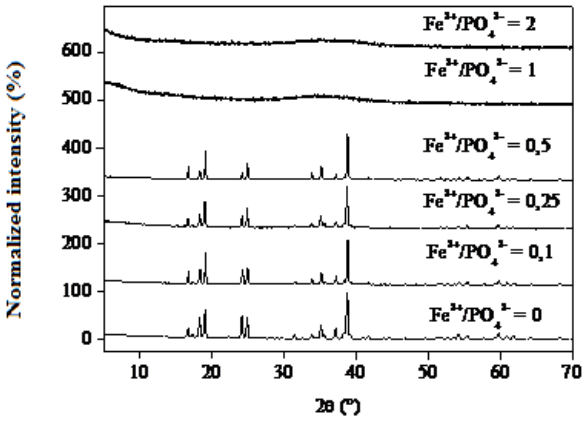

Fig. 14. Superposition of X-rays diffractograms of precipitates obtained for different Fe^{3+}/PO_4^{3-} molar ratios

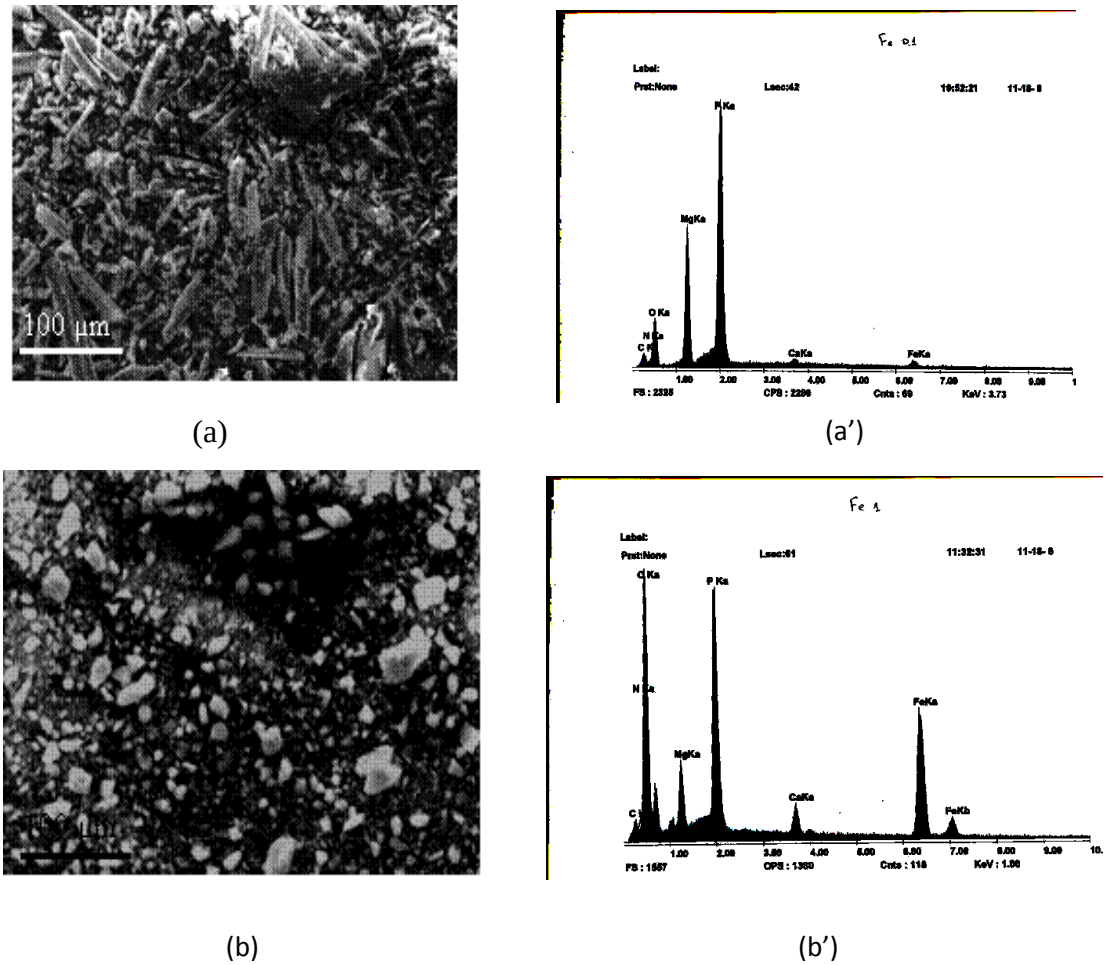

Fig. 15. EDAX spectra and SEM of precipitates obtained for different Fe^{3+}/PO_4^{3-} molar ratios

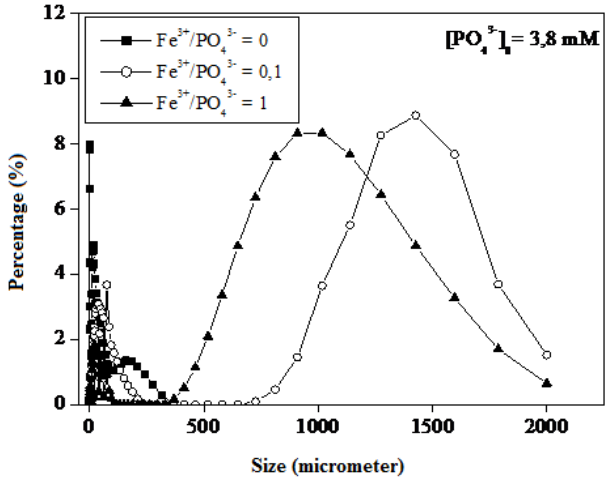

Fig. 16. Percentage of particle size of precipitates obtained for different Fe^{3+}/PO_4^{3-} molar ratios

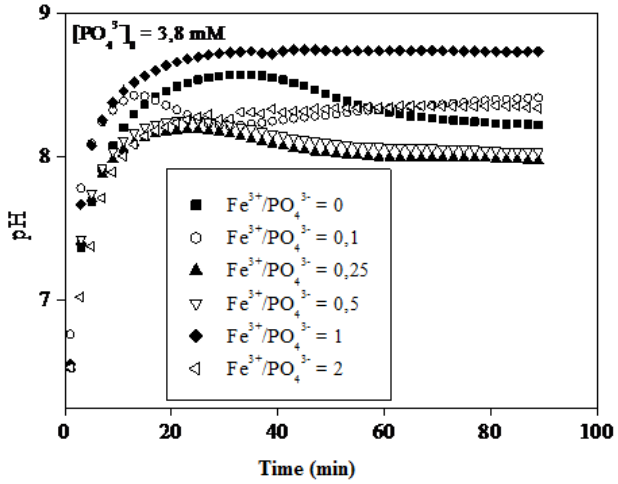

Fig. 17. Temporal evolution of solution pH for different Fe^{3+}/PO_4^{3-} molar ratios.

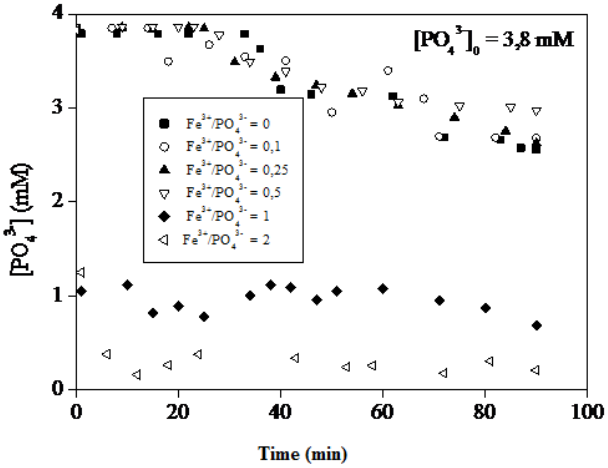

Fig. 18. Temporal evolution of phosphates ions concentration for different Fe^{3+}/PO_4^{3-} molar ratios

Table 1. Induction time, pH of precipitation and, phosphates ions removal for different Fe^{3+}/PO_4^{3-} molar ratios

Fe^{3+}/PO_4^{3-} molar ratio	Induction time t_i (min)	pH of précipitation	Phosphates ions removal (%)
0	35	8.57	32.55
0.1	14	8.44	30.38
0.25	24	8.19	31.38
0.5	23	8.26	23.04
1	< 1	6.5	82.06
2	< 1	6.5	94.51

CONCLUSION

Increasing the calcium ions in the solution improved the phosphate removal efficiency and leads to the evolution of the precipitate solid from crystalline phase (struvite) to an amorphous phase (calcium phosphate: $Ca_9(PO_4)_6 \bullet nH_2O$) from Ca^{2+} concentration of 4 mM. Nevertheless, the formation of the amorphous phase preceded the struvite ones in the range of Ca^{2+} concentration between 2.5 to 3.5 mM. The increase in Ca^{2+} ions in the solution from 2 to 4 mM approaches a homogeneous distribution of the average particle size. Moreover, the particles average size of the amorphous phase was lower than that of the crystallized (struvite) phase. However, their average ratio is greater than that of struvite.

Increasing the concentration of K^+ improved phosphate removal yield and does not affect the purity of the struvite obtained. Furthermore, another phase not detected by X-ray diffraction containing such ions could co-precipitate with struvite because of the appearance of this element in the analysis of samples by EDAX.

The introduction of iron ions Fe^{3+} in the solution caused huge change both, on physicochemical parameters, and on the morphology of the precipitate obtained. Indeed, the increase in the molar ratio destroyed struvite crystallization immediately and formed an amorphous phase:

(iron phosphate: $FePO_4 \bullet 2H_2O$) at pH 6.5 and $\frac{Fe^{3+}}{PO_4^{3-}} \geq 1$.

Furthermore, the presence of iron promoted increasing of particles size of the two phases (crystalline and amorphous).
It should be noted that the yield of phosphate removal is better when forming the amorphous phase. It decomposed, into one step, under the effect of temperature and disadvantages scaling.

ACKNOWLEDGEMENTS

This work was supported by the Natural water treatment laboratory (Research and technology centre of water, technopark of Borj Cedria, Tunisia) directed by Professor Mohamed Ben Amor and University of Maradi directed by Professor Mahamane Saadou. That all centre and Maradi University staff receives here my gratitude.

REFERENCES

Banu M (2005). Mise en forme d'apatites nanocristallines : céramiques et ciments. Thèse de doctorat INP : Science et Génie des Matériaux, Toulouse.

Ben Moussa S, Tlili MM, Batis N, Ben Amor M (2011). Influence of temperature on struvite precipitation by CO_2-degassing method. Crystal Research and Technology 46: 255-260.

Borgerding J (1972). Phosphate deposits in digestion systems. Journal of Water Pollut. Control Fed. 44: 813–819.

Bridger G (2001). Fertilizer value of struvite. CEEP Scope Newsletter 43: 3-4.

De-Bashan LE, Bashan Y (2004). Recent advances in removing phosphorus from wastewater and its future use as fertilizer. Water Research 36: 4222-4246.

Diwani GE, Rafie SE, Ibiari NNE, Aila HIE (2007). Recovery of ammonia nitrogen from industrial wastewater treatment as struvite slow releasing fertilizer. Desalination. 214: 200–214.

Heughebaert JC, Montel G (1977). Etude de l'évolution de l'orthophosphate tricalcique non cristallin en phosphate apatitique à la faveur d'une réaction chimique à température ordinaire. Revue de Physique Appliquée 12 : 691-694.

Huang H, Xiao D, Xhang Q, Ding L (2014a). Removal of ammonia from landfill leachate by struvite precipitation with the use of low-cost phosphate and magnesium sources. Journal of Environmental Management 14: 191-198.

Huang H, Chen Y, Jiang Y, Ding L (2014b). Treatment of swine wastewater combined with MgO-saponification wastewater by struvite precipitation technology. Chemical Engineering Journal 254: 418-425.

Hutnik N, Kozik A, Mazienczuk A, Boguslawa W, Piotrowsky K, Matynia A (2013). Phosphates (V) recovery from phosphorus mineral fertilizers industry wastewater by continuous struvite reaction crystallization process. Water Research 47: 3635-3643.

Kabdasli I, Parsons SA, Tunay O (2006). Effect of major ions on induction time of struvite precipitation. Croat. Chem. Acta 79 : 243-251.

Kozik A, Hutnik N, Piotrowsky K, Matynia A (2014). Continuous reaction crystallization of struvite from diluted aqueous solution of phosphate (V) ions in the presence of magnesium ions excess. Chemical Engineering Research and Design 92: 481-490.

Lahav O, Telzhensky M, Zewuhn A, Gendel Y, Gerth J, Calmano W, Birnhack L (2013). Struvite recovery from municipal-wastewater sludge centrifuge supernatant using seawater NF concentrate as a cheap Mg (II) source. Separation and Purification Technology 108: 103-110.

Le Corre KS, Valsami-Jones E, Hobbs P, Parsons SA (2005). Impact of calcium on struvite crystal size, shape and purity. Journal of Crystal Growth 283: 514-522.

Mudragada R, Kundral S, Coro E, Moncholi ME, Laha S, Tansel B (2014). Phosphorus removal during sludge dewatering to prevent struvite formation in sludge digesters by full scale evaluation. Journal of Water Process Engineering 2: 37-42.

Muryanto S, Bayuseno AP (2014). Influence of Cu^{2+} and Zn^{2+} as additives on crystallization kinetics and morphology of struvite.

Powder Technology 25: 602-607. 21. Walleys R (1952). Ann. Chim., 12 série 7 : 808-848.

Saidou H, Korchef A, Ben Moussa S, Ben Amor M (2009a). Struvite precipitation by the dissolved CO_2 degasification technique: Impact of the airflow rate and pH. Chemosphere 74: 338-343.

Saidou H, Ben Moussa S, Ben Amor M (2009b). Influence of airflow rate and substrate nature on heterogeneous struvite precipitation. Environmental Technology 30: 75-83.

Saidou H, Trabelsi I, Ben Amor M (2010). Phosphorus removal from Tunisian landfill leachate through struvite precipitation under controlled degassing technique. Desalination and Water Treatment. 21: 295-302.

Webb KM, Ho GE (1992). Struvite ($MgNH_4PO_4 \cdot 6H_2O$) solubility and its application to a piggery effluent problem. Water Sci. Technol. 26: 2229–2232.

Ye Z, Shen Y, Zhang Z, Chen S, Shi J (2014). Phosphorus recovery from wastewater by struvite crystallization: Property of aggregates. Journal of Environmental Sciences 26: 991-1000.

Zahidi E (1984). Etude du système phosphate de calcium-Amino, 2 éthyl phosphate de calcium, en milieu eau/éthanol. Thèse d'état INP : Physico-Chimie des Matériaux, Toulouse.

Zahidi E, Lebugle A, Bonel G (1985). Sur une nouvelle classe de matériaux pour prothèses osseuses ou dentaires. Bull. Soc. Chim. Fr. 4 : 523-527.

Zhang T, Ding L, Ren H, Xiong X (2009). Ammonium nitrogen removal from cooking wastewater by chemical precipitation recycle technology. Water Research 43: 5209–5215.

Zhang T, Ding L, Ren H, Guo Z, Tan J (2010). Thermodynamic modelling of ferric phosphate precipitation for phosphorus removal and recovery from wastewater. Journal of Hazardous Materials 176: 444-450.